Neuro-Oncology
19(6), 808–819, 2017 | doi:10.1093/neuonc/now267 | Advance Access date 30 December 2016

Defining the temporal course of murine neurofibromatosis-1 optic gliomagenesis reveals a therapeutic window to attenuate retinal dysfunction

Joseph A. Toonen, Yu Ma, and David H. Gutmann

Department of Neurology, Washington University School of Medicine (WUSM), St Louis, Missouri (J.A.T., Y.M., D.H.G.)

Corresponding Author: David H. Gutmann, MD, PhD, Department of Neurology, Washington University, Box 8111, 660 S. Euclid Avenue, St. Louis MO 63110 (gutmannd@wustl.edu).

Abstract

Background. Optic gliomas arising in the neurofibromatosis type 1 (NF1) cancer predisposition syndrome cause reduced visual acuity in 30%–50% of affected children. Since human specimens are rare, genetically engineered mouse (GEM) models have been successfully employed for preclinical therapeutic discovery and validation. However, the sequence of cellular and molecular events that culminate in retinal dysfunction and vision loss has not been fully defined relevant to potential neuroprotective treatment strategies.

Methods. *Nf1*$^{flox/mut}$ GFAP-Cre (FMC) mice and age-matched *Nf1*$^{flox/flox}$ (FF) controls were euthanized at defined intervals from 2 weeks to 24 weeks of age. Optic nerve volumes were measured, and optic nerves/retinae analyzed by immunohistochemistry. Optical coherence tomography (OCT) was performed on anesthetized mice. FMC mice were treated with lovastatin from 12 to 16 weeks of age.

Results. The earliest event in tumorigenesis was a persistent elevation in proliferation (4 wk), which preceded sustained microglia numbers and incremental increases in S100+ glial cells. Microglia activation, as evidenced by increased interleukin (IL)-1β expression and morphologic changes, coincided with axonal injury and retinal ganglion cell (RGC) apoptosis (6 wk). RGC loss and retinal nerve fiber layer (RNFL) thinning then ensued (9 wk), as revealed by direct measurements and live-animal OCT. Lovastatin administration at 12 weeks prevented further RGC loss and RNFL thinning both immediately and 8 weeks after treatment completion.

Conclusion. By defining the chronology of the cellular and molecular events associated with optic glioma pathogenesis, we demonstrate critical periods for neuroprotective intervention and visual preservation, as well as establish OCT as an accurate biomarker of RGC loss.

Key words

optic glioma | optical coherence tomography | pediatric brain tumor | retinal ganglion cell | retinal nerve fiber layer

Individuals with the neurofibromatosis type 1 (NF1) inherited cancer syndrome are prone to the development of benign and malignant tumors. In children, the two most common tumors are the benign peripheral nerve sheath tumor (plexiform neurofibroma) and the central nervous system optic pathway glioma (OPG). OPGs arise in 15%–20% of children with NF1, where they most frequently form within the optic nerves and optic chiasm in children younger than 7 years.[1] Since these tumors occur within the optic pathway, 30%–50% of children with NF1-OPG will experience a decline in visual acuity,[2] which frequently prompts chemotherapy.

Unfortunately, it is often difficult to reliably measure visual acuity in preverbal children with comorbid attention deficits, hyperactivity, and behavioral problems, as is commonly seen in individuals with NF1.[3,4] While behavior-based measures of visual acuity have been successfully employed for therapeutic decision making, optical coherence tomography (OCT)

Importance of the study

Vision loss represents the most significant clinical consequence of optic glioma progression in children with NF1. In order to identify critical temporal windows for neuroprotective intervention, we defined the chronology of cellular and molecular events that underlie *Nf1* optic glioma development and vision loss in an authenticated GEM model. In addition, we show that OCT is an accurate indicator of RGC loss in *Nf1* optic glioma–bearing mice. Moreover, we demonstrate that lovastatin treatment can halt further retinal dysfunction two months after the completion of drug therapy. Collectively, this study establishes the foundations for future investigations in mice aimed at ameliorating progressive visual decline in children with NF1-associated optic glioma.

has recently been used as an indirect measure of retinal dysfunction.[5] OCT quantifies the thickness of the retinal nerve fiber layer (RNFL), which contains the retinal ganglion cell (RGC) axons that course through the optic nerve to the lateral geniculate body. While this objective measure would mitigate the confounding issue of behavior and patient compliance, it is not possible to determine how this indirect measurement of RNFL thickness correlates with actual retinal histopathology in children with NF1-OPG, or to establish a clear temporal relationship between tumorigenesis and tumor-induced vision loss in affected individuals.

With the development of credentialed genetically engineered mouse (GEM) models of NF1-optic glioma,[6,7] the chronological sequence of cellular and molecular events can be defined, beginning with tumor formation and culminating in RGC loss and RNFL thinning. One such *Nf1* GEM strain (*Nf1*$^{flox/mut}$; GFAP-Cre, FMC mice) develops low-grade gliomas of the prechiasmatic optic nerve and chiasm by 12 weeks of age with >90% penetrance. The resulting tumors, similar to their human counterparts, exhibit low proliferative indices, increased microglial numbers, nuclear pleiomorphism, and cellular atypia,[8] and can be visualized by neuroimaging.[9] In addition, mice harboring these gliomas exhibit axonal swelling, RGC death, and RNFL thinning at 3 months of age,[10,11] but only demonstrate reduced visual acuity at 6 months of age as detected by visual optokinetic system testing.[12]

Herein, we performed a detailed analysis of the natural history of optic glioma formation and retinal dysfunction in FMC mice in order to identify critical periods for neuroprotective intervention, and establish OCT as an accurate biomarker of RGC loss. Importantly, we demonstrate that lovastatin halts further RGC loss and RNFL thinning immediately and 2 months following treatment cessation.

Materials and Methods

Mice

FMC and age-matched *Nf1*$^{flox/flox}$ (FF) (wild-type control) littermate mice were maintained on a C57BL/6 background.[7] Similar numbers of males and females were used for histological optic nerve comparisons; however, only female mice were used for retinal analyses, since *Nf1* optic glioma–induced vision loss is only observed in female mice.[12] Mice were euthanized at predetermined ages with at least 6 mice per group (FF/FMC). All mouse experiments were approved by the WUSM Institutional Animal Care and Use Committee.

Ten mice each were treated with 10 mg/kg/day lovastatin (dissolved in 1% methylcellulose) or vehicle by oral gavage for 4 weeks (5 d/wk), beginning at 12 weeks of age, and euthanized immediately after treatment cessation or 8 weeks later.

Approximately 0.75 mL of blood was collected by cardiac puncture from anesthetized mice using 23–25 gauge needles and heparin-coated syringes.

Chiasms and optic nerves were microdissected, imaged using a Leica DFC 3000G camera in Leica application suite A, and volumes determined as previously published.[13]

Murine eyes and optic nerves were prepared for sectioning and immunostaining using specific antibodies (Supplementary Table S1) as previously described.[14]

Optical Coherence Tomography

Mice were anesthetized with an intraperitoneal injection of 50 mg/kg ketamine-HCl and 7 mg/kg xylazine. Pupils were dilated with tropicamide/phenylephrine eye drops, while artificial tears were used to prevent corneal desiccation. Spectral domain (SD)-OCT was performed on the Bioptigen system using a custom lens. A 2 × 2 mm rectangular scanning pattern was employed to obtain 100 horizontal B-scans, each comprising 1000 A-scans centered on the optic nerve head. Measurements of RNFL and inner plexiform layer–ganglion cell layer (IPL-GCL) thicknesses were performed with InVivoVue software.

Quantitative Real-Time PCR and Enzyme-Linked Immunosorbent Assay

Optic nerves microdissected following Ringer's solution perfusion were placed in RNAlater (Life Technologies) and RNA isolated using the RNeasy mini-kit (Qiagen) for cDNA generation with the Superscript III first strand synthesis system (Life Technologies). Quantitative (q)PCR was performed using the Bio-Rad CFX96 Real-Time System with SYBR-Green detection and predesigned qPCR primers (Integrated DNA Technologies). Fold expression changes were calculated using the ΔΔCT method. Serum (1:5 dilution) was assayed using the phosphorylated neurofilament heavy chain (pNF-H) version 1 enzyme-linked immunosorbent assay kit (EnCor Biotechnology).

Statistical Analysis

Analyses were performed using GraphPad Prism software. The number of Brn3a+ cells per 20× image field was converted to a percentage using the arithmetic mean of Brn3a+ cells in each cohort of FF mice. Student's *t*-tests were used to determine significant differences ($P \leq .05$) between FMC and FF (control) groups at each time point.

Results

Increased Proliferation Is the Earliest Event in *Nf1* Optic Gliomagenesis

Proliferative indices (%Ki67+ cells) were elevated in both FF and FMC mice at 2 weeks of age, but were not significantly different from each other (FF, 6.79% ± 1.02; FMC 7.49% ± 1.08; $P = .65$; Fig. 1A). At 4 weeks of age, increased proliferation was first detected in FMC mice relative to controls (FF, 0.59% ± .26; FMC 1.3% ± 0.19; $P = .049$; Fig. 1A), which continued to rise at 6 weeks of age (FF, 0.2% ± 0.07; FMC 1.42% ± 0.37; $P = .009$), 9 weeks (FF, 0.44% ± .22; FMC 2.24% ± .43; $P = .039$), and 12 weeks of age (FF, 0.2% ± 0.07; FMC 1.42% ± 0.37; $P = .009$) in FMC mice (Fig. 1A). However, after 12 weeks of age, proliferation remained similarly elevated relative to controls (16 wk: FF, 0.06% ± 0.06; FMC 1.43% ± 0.42; $P = .014$; 24 wk: FF, 0.44% ± 0.22; FMC 2.02% ± 0.40; $P = .011$; Fig. 1A).

In addition to the macroglial cells (astrocytes) that comprise the bulk of the tumor cells, microglia are also critical for *Nf1* optic glioma formation and maintenance.[15–17] While similar percentages of Iba1+ cells were found at 2 and 4 weeks in FF and FMC mice, the number of microglia decreased in FF mice after 4 weeks of age, but remained elevated at similar levels between 4 and 24 weeks of age in FMC optic nerves (Fig. 1B). The Iba1+ cells were amoeboid-shaped in FF and FMC optic nerves at 2 and 4 weeks of age. However, at subsequent time points in FF mice, these cells became ramified, suggestive of a resting or inactive state, while those in FMC mice remained amoeboid, indicative of monocyte activation (Fig 1C).

Proliferating neoplastic cells in the optic nerves of FMC mice are thought to give rise to the tumoral astrocytes, which comprise the largest cell population within the glioma.[7] While increased glial fibrillary acidic protein–positive (GFAP+) cell (astrocyte) immunoreactivity is a feature of both mouse and human NF1 optic gliomas,[7] quantitating the number of GFAP+ cells is challenging due to the predominant labeling of astrocytic processes. For this reason, in conjunction with GFAP immunohistochemistry (Fig. 2A), we employed S100β staining to quantitate the number of immunopositive glial cell bodies.[8] In contrast to the increase in Ki67+ cells, no discernible increases in S100β+ cells were observed at 2 or 4 weeks of age (Fig. 2B). Instead, increased astroglial numbers were first observed at 6 weeks of age (FF, 36.77% ± 1.7; FMC 49.6 ± 4.21; $P = .0279$), which rose at 9 (FF, 35.42% ± 3.57; FMC 63.20 ± 2.94; $P = .001$), 12 (FF, 38.85% ± 2.1; FMC 64.72 ± 1.02; $P = .0001$), 16 (FF, 34.10% ± 2.41; FMC 66.07 ± 2.47; $P = .01$), and 24 (FF, 24.86% ± 6.3; FMC 58.56 ± 3.9; $P = .005$) weeks of age in FMC mice relative to FF controls.

Finally, architectural distortion (optic nerve volume enlargement) was not apparent before 9 weeks of age (2 wk: FF, mean = .039 mm^3 ± 0.002 [SEM]; FMC, 0.034 mm^3 ± 0.004; $P = .25$; 4 wk: FF, 0.046 mm^3 ± 0.002; FMC 0.052 mm^3 ± 0.002; $P = .11$; 6 wk: FF, 0.032 mm^3 ± 0.001; FMC 0.039 mm^3 ± 0.003; $P = .3$; Fig. 2C). At 9 weeks of age, a 1.26-fold increase (FF, 0.056 mm^3 ± 0.005; FMC 0.071 mm^3 ± 0.005; $P = .04$) in optic nerve volume was observed (Fig. 2C). This volume differential continued to increase in FMC mice (FF, 0.056 mm^3 ± 0.005; FMC, 0.071 mm^3 ± 0.005; 1.42-fold; $P = .04$), eventually plateauing at 16 (FF, 0.056 mm^3 ± 0.004; FMC, 0.088 mm^3 ± 0.006; $P = .0006$) and 24 (FF, 0.057 mm^3 ± .003; FMC, 0.098 mm^3 ± 0.004; $P = .0001$) weeks of age.

Collectively, these data elucidate a temporal sequence of events that begins with increased proliferation, followed by increased astroglial and microglial cell numbers, and culminating in optic glioma formation.

Axonal Injury and Apoptosis Are the Earliest Events in Retinal Dysfunction

Axonal swelling within the optic nerves was previously associated with RGC death in FMC mice,[10] suggesting early axonal injury, which might best be detected using a more sensitive indicator of neuronal damage. Phosphorylated NF-H demarcates axonal injury in murine models of nervous system damage,[18] including *Nf1* optic glioma.[19] Supporting increased pNF-H immunoreactivity as a marker of axonal injury, we observed increased pNF-H immunostaining at 6 weeks of age. At 16 and 24 weeks of age, pNF-H staining decreased relative to 12 weeks, and decreased further at 24 weeks of age (Fig. 3A).

Terminal deoxynucleotidyl transferase deoxyuridine triphosphate nick end labeling (TUNEL) was next performed to determine when RGC death was first detected. Whereas no change in RGC apoptosis was detected at 2 (FF, 5.73% ± 0.79; FMC, 6.14% ± 0.37; $P = .78$) or 4 (FF, 1.33% ± 0.57; FMC, 1.54% ± 0.63; $P = .82$) weeks of age in FMC mice relative to FF controls, an increased proportion of TUNEL+ cells in the GCL was first observed at 6 weeks of age in FMC mice (FF, 2.52% ± 0.55; FMC, 7.25% ± 0.83; $P = .009$; Fig. 3B). This increase peaked between 9 and 16 weeks of age (9 wk: FF, 1.69 ± 0.53; FMC, 7.23% ± 0.39; $P = .001$; 12 wk: FF, 1.89% ± 0.76; FMC, 11.46% ± 1.84; $P = .0001$; 16 wk: FF, 1.86% ± 0.74; FMC, 9.67% ± 1.21; $P = .0005$), but decreased by 24 weeks of age (FF, 5.94% ± 0.75; FMC, 9.54% ± 1.09; $P = .027$).

To quantify RGC loss, we used Brn3a to identify RGCs within the GCL.[20] While no decrease in Brn3a+ cells was observed in FMC mice at 2 (FF, 100% ± 5.35; FMC, 101.1% ± 2.29; $P = .87$), 4 (FF, 100% ± 7.79; FMC, 99.55% ± 8.75; $P = .97$), or 6 (FF, 100% ± 7.31; FMC, 99.25% ± 4.66; $P = .93$) weeks relative to FF controls, RGC loss was first detected at 9 weeks (FF, 100% ± 6.55; FMC, 77.66% ± 4.55; $P = .016$), and continued to decline thereafter (12 wk: FF, 100% ± 8.81; FMC, 67.8% ± 5.39; $P = .014$; 16 wk: FF, 100% ± 4.52; FMC, 67.26% ± 3.43; $P = .0001$; 24 wk: FF, 100% ± 4.9; FMC, 44.74% ± 3.84; $P = .0001$; Fig. 3C).

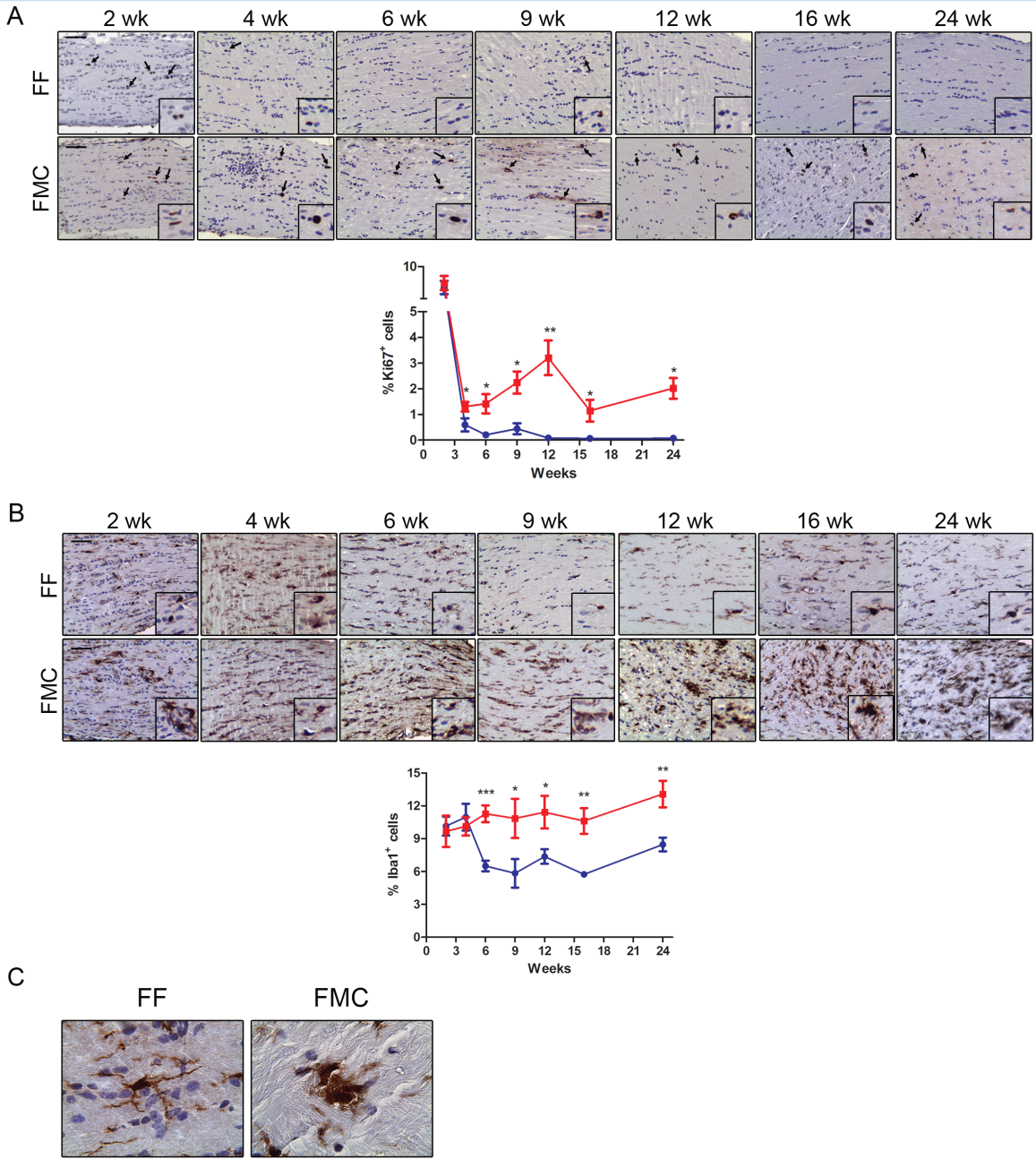

Fig. 1 Increased proliferation and microglia are detected at 6 weeks of age in FMC mice. (A) Increased percentages of Ki67+ cells were observed in FMC relative to FF optic nerves, beginning at 4 weeks, and increasing from 6 to 12 weeks of age. The %Ki67+ cells subsequently decreased, but remained higher in FMC relative to FF optic nerves at 16 and 24 weeks. (B) The %Iba1+ cells (microglia) remained unchanged in FMC mice beginning at 6 weeks of age and beyond, whereas decreased numbers of microglia were observed in FF mice after 6 weeks of age. At least 6 mice per group were included for each time point. (C) Microglia in FF mice were ramified with elongated processes, while those in FMC mice exhibited amoeboid morphologies. Blue lines = FF, red lines = FMC, $*P \leq .05$, $**P \leq .01$, $***P \leq .001$. Graph denotes mean ± SEM. Scale bars = 50 μm.

OCT Is an Accurate Biomarker of Optic Glioma–Induced RGC Neuronal Injury

The temporal course of retinal pathology in the setting of *Nf1* murine optic glioma development suggests that two potential biomarkers might be useful indicators of tumor-induced visual impairment (serum pNF-H levels and RNFL thickness). Based on previous studies in amyotrophic lateral sclerosis and traumatic brain injury,[21,22] we explored the possibility that serum pNF-H levels might correlate with axonal injury in FMC mice relative to FF controls at various time points. Unfortunately, there was no correlation between pNF-H serum levels and optic glioma presence or continued growth at any

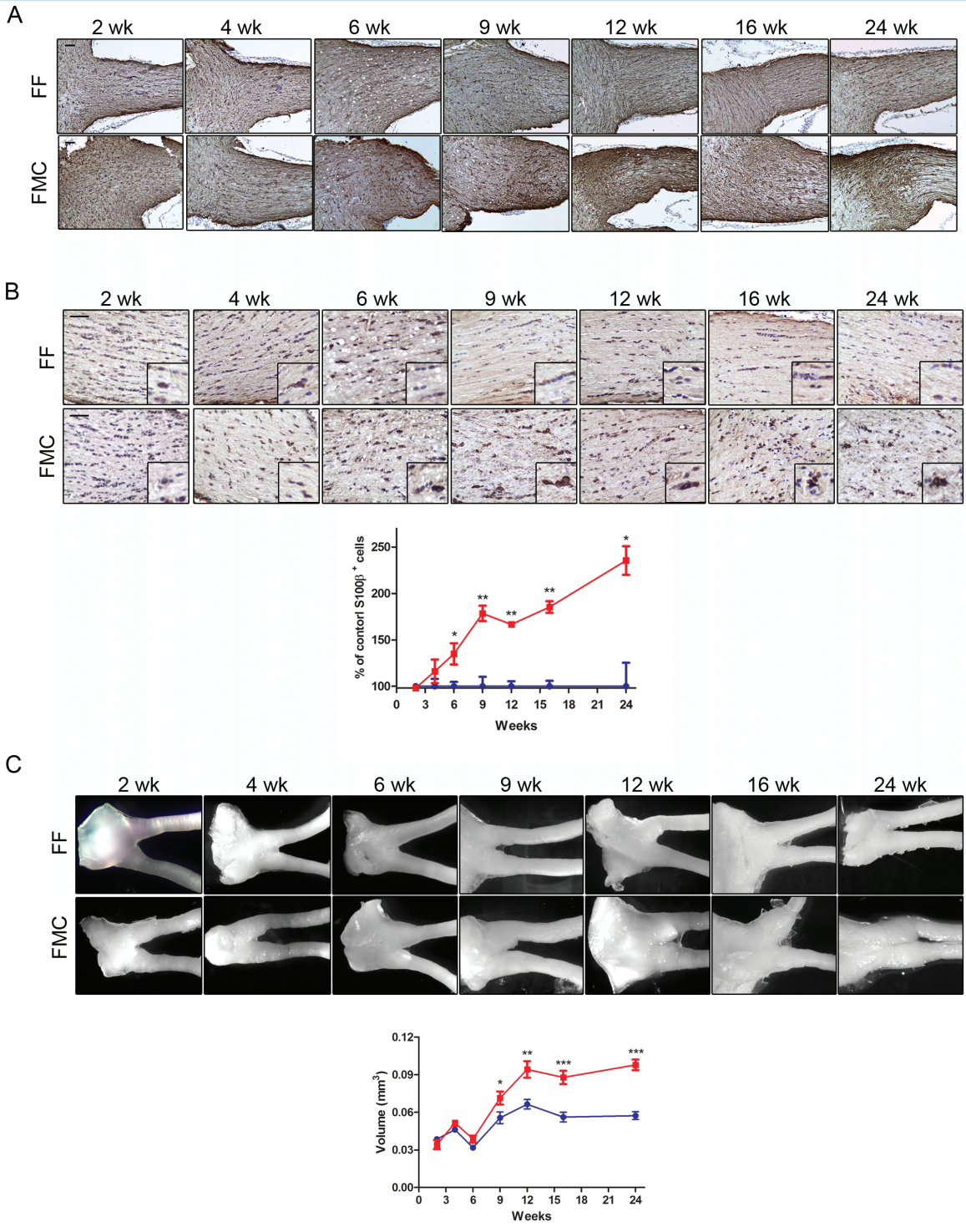

Fig. 2 Temporal progression of tumor formation in FMC mice. (A) GFAP immunostaining increased over time in FMC compared with FF optic nerves. (B) Increased percentages of S100β+ astrocytes were observed in FMC relative to FF optic nerves by 6 weeks of age, expressed as the %S100β+ cells relative to FF controls. S100β+ cells continued to increase thereafter. (C) Optic nerves and corresponding optic nerve volumes increased in FMC mice between 9 weeks and 12 weeks of age ($n = 8$). At least 6 mice per group were included for each time point. Blue lines = FF, red lines = FMC, $^{*}P \leq .05$,$^{**}P \leq .01$, $P \leq .001$. Graph denotes mean ± SEM.

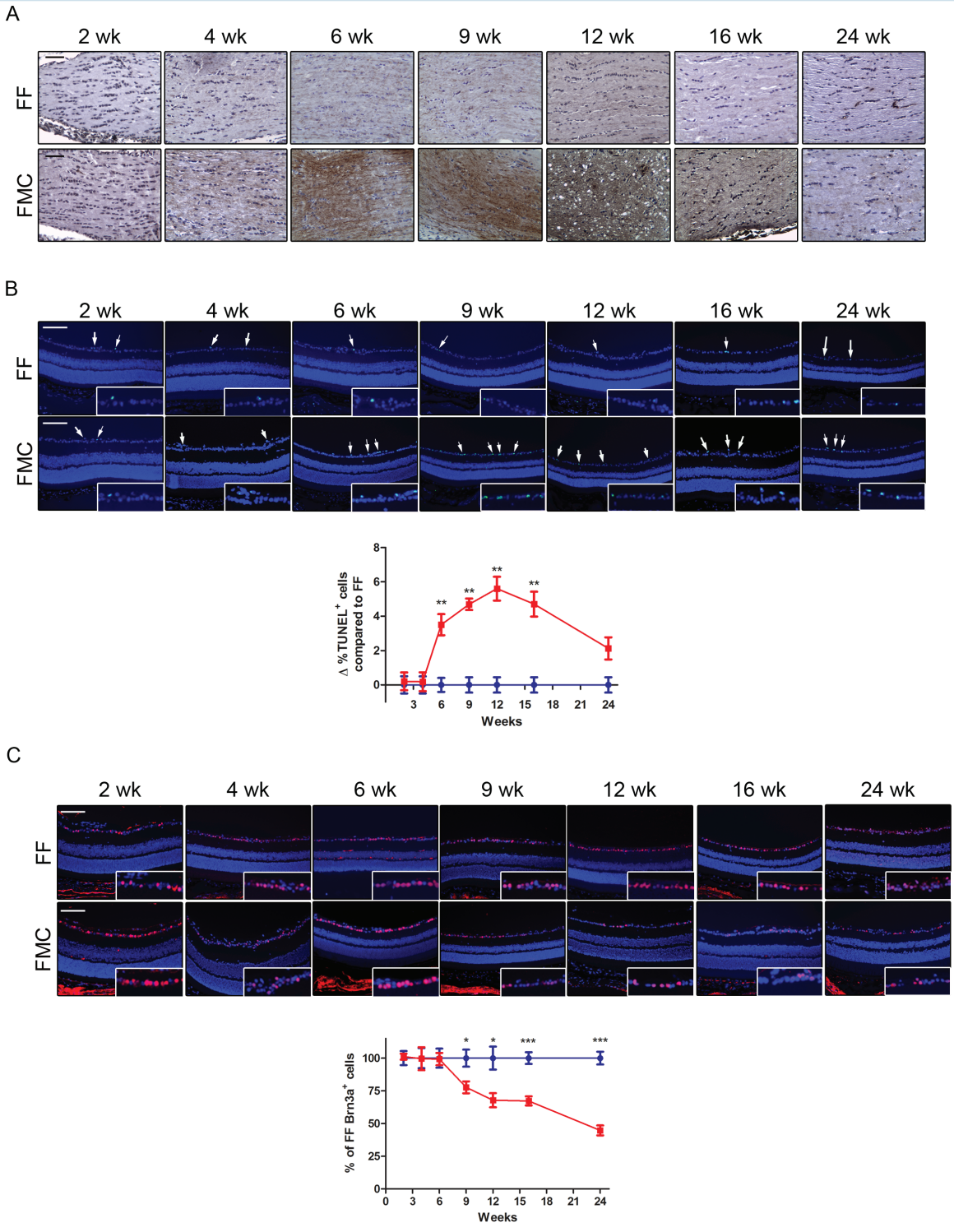

Fig. 3 Axonal injury coincides with RGC death. (A) Phosphorylated NF-H staining reveals axonal damage by 6 weeks of age, which gradually decreases at 16 and 24 weeks in FMC relative to FF mice. (B) An increase in %TUNEL+ cells was observed by 6 weeks of age in FMC mice, which further increased at 9 and 12 weeks of age, before declining. Data represent a change from the mean %TUNEL+ cells in FF mice at each time point. (C) Brn3a+ cell (RGCs) loss begins at 9 weeks of age in FMC mice; 100% denotes the mean number of Brn3a+ cells in FF mice at each time point. At least 6 mice per group were included for each time point. Blue lines = FF, red lines = FMC, $*P \leq .05$,$**P \leq .01$, $P \leq .001$. Graph denotes mean ± SEM. Scale bars = 50 μm.

time point (Supplementary Fig. S1), excluding serum pNF-H levels as a clinically relevant biomarker of optic nerve damage.

Since SD-OCT has emerged as a useful tool to monitor RNFL and IPL-GCL thickness in children with sporadic and NF1-associated OPG,[23] we measured the thickness of these retinal layers as a function of time in live animals,[24] beginning at 6 weeks of age. While no differences were observed in IPL-GCL (FF, 6.07 μm ± 0.22; FMC, 6.29 μm ± 0.31; $P = .59$) or RNFL (FF, 2.8 μm ± 0.07; FMC, 2.38 μm ± 0.15; $P = .07$) thickness in FMC mice at 6 weeks of age relative to controls, progressive loss of both IPL-GCL and RNFL thickness started at 9 weeks (IPL: FF, 6.22μm ± 0.23; FMC, 5.0 μm ± 0.18; $P = .0056$; RNFL: FF, 3.28 μm ± 0.17; FMC, 1.91 μm ± 0.20; $P = .002$), where it further declined at 12 (IPL: FF, 5.81 μm ± 0.56; FMC, 4.7 μm ± 0.21; $P = .05$; RNFL: FF, 2.58 μm ± 0.09; FMC, 1.81 μm ± 0.04; $P = .0003$), 16 (IPL: FF, 5.9 μm ± 0.22; FMC, 4.5 μm ± 0.17; $P = .0013$; RNFL: FF, 3.12 μm ± 0.39; FMC, 1.52 μm ± 0.15; $P = .002$), and 24 weeks of age (IPL: FF, 5.3 ± 0.23 μm; FMC, 4.43 μm ± 0.17; $P = .043$; RNFL: FF, 2.5 μm ± 0.19; FMC, 1.21 μm ± 0.12; $P = .0054$) (Fig. 4A–D). Similar to previous studies comparing histological and OCT measurements in mice,[24] we found a strong correlation between direct SMI-32 measurements and RNFL measurements obtained using SD-OCT (Fig. 4E), as well as between RNFL thickness and RGC loss (Fig. 4F). Moreover, when a 7.5-micron RNFL thickness or lower cutoff was used, 11 of 12 mice (92%) exhibited ≥30% decreases in RGC numbers relative to FF mice, whereas those with RNFL thicknesses of >7.5 microns were more likely to have less than a 30% decrease in RGC numbers (11/14 mice, 79%). These data support the use of OCT as a biomarker of IPL-GCL and RNFL integrity prior to loss of visual acuity in mice.

Lovastatin Treatment Ameliorates Further Declines in Retinal Dysfunction

Based on this temporal course of cellular and molecular events, there exists a defined interval between the onset of apoptosis/RNFL thinning and significant RGC loss (>30% reduction in Brn3a+ cells). In this regard, 25%–35% of the RGCs can be lost before a significant decline in visual acuity ensues.[25]This window suggests that death signals produced by cells in the tumor might initiate a sequence of events that culminate in vision loss, and could potentially be interrupted if treatment occurred within this critical time interval.

We first sought to determine whether inflammatory chemokines, like interleukin-1-beta (IL-1β) and tumor necrosis factor-alpha (TNF-α), previously reported to trigger apoptotic pathways in neurons,[26] were elevated in the FMC optic nerves relative to controls. Using qPCR, we observed no differences in *Tnf* RNA expression between FMC and FF mice at 3 months of age (data not shown). However, *Il1b* RNA expression was elevated 3.2-fold in FMC optic nerves relative to FF controls (Fig. 5A). While microglia are the major source of IL-1β in murine *Nf1* optic gliomas, astroglial cells also produce IL-1β in this setting (Supplementary Fig. S2).

We next performed IL-1β immunostaining at time points extending from 2 weeks through 24 weeks. While no differences in IL-1β expression were observed at 2 and 4 weeks of age, the percent of IL-1β+ cells was elevated in the FMC optic nerves relative to FF mice, beginning at 6 weeks of age (FF, 6.62% ± 3.02; FMC, 36.69% ± 9.53; $P = .01$), peaking at 12 weeks (FF, 7.37% ± 2.9; FMC, 48.22% ± 6.72; $P = .005$), and declining thereafter (Fig. 5B). Unfortunately, there is a paucity of IL-1β inhibitors available for preclinical study, and the one nonspecific inhibitor commercially available (VX-765) had no effect on *Nf1* mouse optic glioma–induced RGC apoptosis in vivo (data not shown).

In order to determine whether treatment of *Nf1* optic glioma (FMC) mice prior to vision loss could attenuate further RGC loss and RNFL thinning, FMC mice were treated at 12 weeks of age when tumor is detectable on MRI and there is RFNL thinning, but less than 30% RGC loss is observed[9] (Fig. 6A). In this manner, we strove to design a preclinical experiment that most closely parallels the setting in which neuroprotective strategies might be implemented in the clinic setting. For these proof-of-concept studies, we chose lovastatin as a nonspecific RAS inhibitor, which blocks RAS signaling in the brains of *Nf1* mutant mice and has been used safely to treat children with NF1-associated learning deficits.[27] Importantly, lovastatin treatment reduces RAS/mechanistic target of rapamycin (mTOR) activation important for *Nf1*-deficient tumor growth, as well as increases RAS-mediated cyclic AMP (cAMP) generation[28] critical for *Nf1+/–* mouse RGC survival.[11] Evidence of target inhibition in FMC mice following lovastatin treatment was demonstrated by an increase in retinal cAMP levels and a reduction in mTOR (phospho-S6) activation in the optic gliomas (Fig 6B).

Mice collected immediately following lovastatin treatment revealed decreased optic nerve volumes (control, 0.10 mm^3 ± 0.007; lovastatin, 0.083 mm^3 ± 0.004; $P = .02$), proliferation (%Ki67+ cells; control, 3.7% ± 0.84; lovastatin, 0.42% ± 0.20; $P = .019$), microglia infiltration (%Iba1+ cells; control, 12.84% ± 3.23; lovastatin, 5.74% ± 1.17; $P = .03$), and IL-1β expression (control, 42.75% ± 6.8; lovastatin, 13.6% ± 3.9; $P \leq .02$) relative to vehicle-treated controls (Fig. 6C). Furthermore, assessment of retinal pathology revealed improved RGC survival by 9.7% (control, 66.26% ± 1.8; lovastatin, 78.96% ± 4.6; $P = .02$) and attenuated RNFL thinning (control, 4.94 μm ± 0.58; lovastatin, 10.1 μm ± 0.63; $P = .03$).

Since children with NF1-OPG will not remain on drug treatments indefinitely, we sought to define the impact of drug cessation on optic nerve and retinal pathology. In these experiments, optic nerves from FMC mice collected 8 weeks after treatment cessation displayed optic nerve volumes (control, 0.011 mm^3 ± 0.009; lovastatin, 0.097 mm^3 ± 0.005; $P = .14$), proliferative indices (control, 1.68% ± 0.26; lovastatin, 1.89% ± 0.79; $P = .79$), and microglia numbers (control, 8.34% ± 0.53; lovastatin, 7.04% ± 0.57; $P = .13$) similar to vehicle-treated controls (Fig. 6D). These results are consistent with previous preclinical experiments using rapamycin, where optic gliomas returned to pretreatment levels within 4 weeks of drug removal.[13] In striking contrast, despite the recurrence of optic gliomas, lovastatin treatment reduced the percent of IL-1β+ cells in the optic nerve (control, 24.68% ± 6.8; lovastatin, 7.58% ± 2.9; $P \leq .05$), as well as further RGC loss and RNFL thinning, such that the percentage of

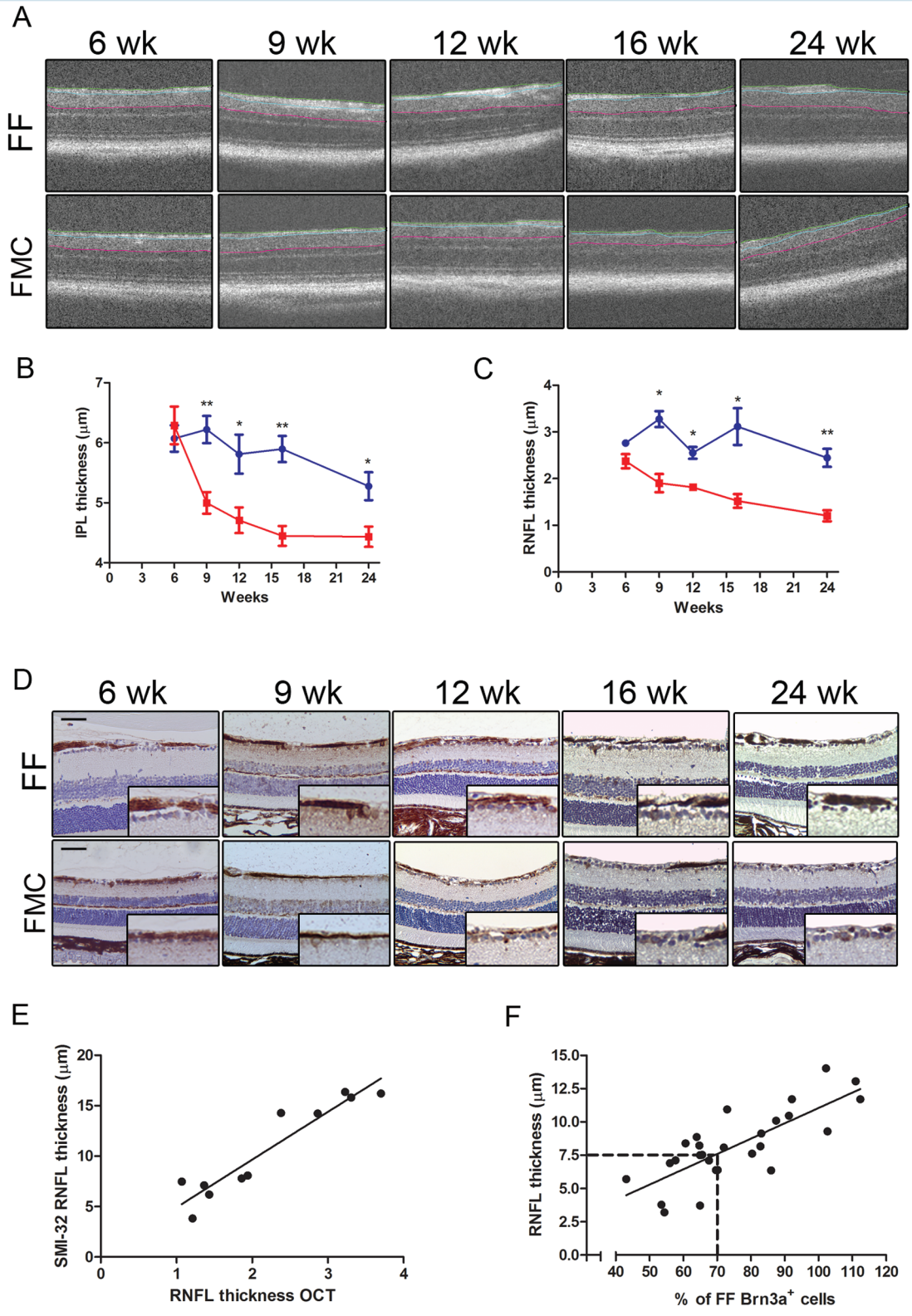

Fig. 4 OCT is an accurate biomarker of IPL-GCL and RNFL thinning. (A) OCT measured RNFL (green to blue line) and IPL-GCL (blue to pink line) thickness. (B) IPL-GCL thinning was first detected by OCT at 9 weeks of age in FMC mice, which progressed through 24 weeks of age. (C) RNFL thickness (OCT) was decreased in FMC mice by 9 weeks of age. (D) SMI-32 staining demonstrated similar results as obtained by OCT. (E) Linear regression scatter plot of SMI-32 and OCT (R^2 = 0.889). (F) Linear regression scatter plot of RGC content and RNFL thinning (R^2 = 0.609). Each data point is represented by comparing direct RNFL measurements with the mean number of Brn3a+ cells in FF mice at each time point. At least 6 mice per group were included for each time point. Blue lines = FF, red lines = FMC, $^*P \leq .05$,$^{**}P \leq .01$, $P \leq .001$. Graph denotes mean ± SEM. Scale bars = 50 μm.

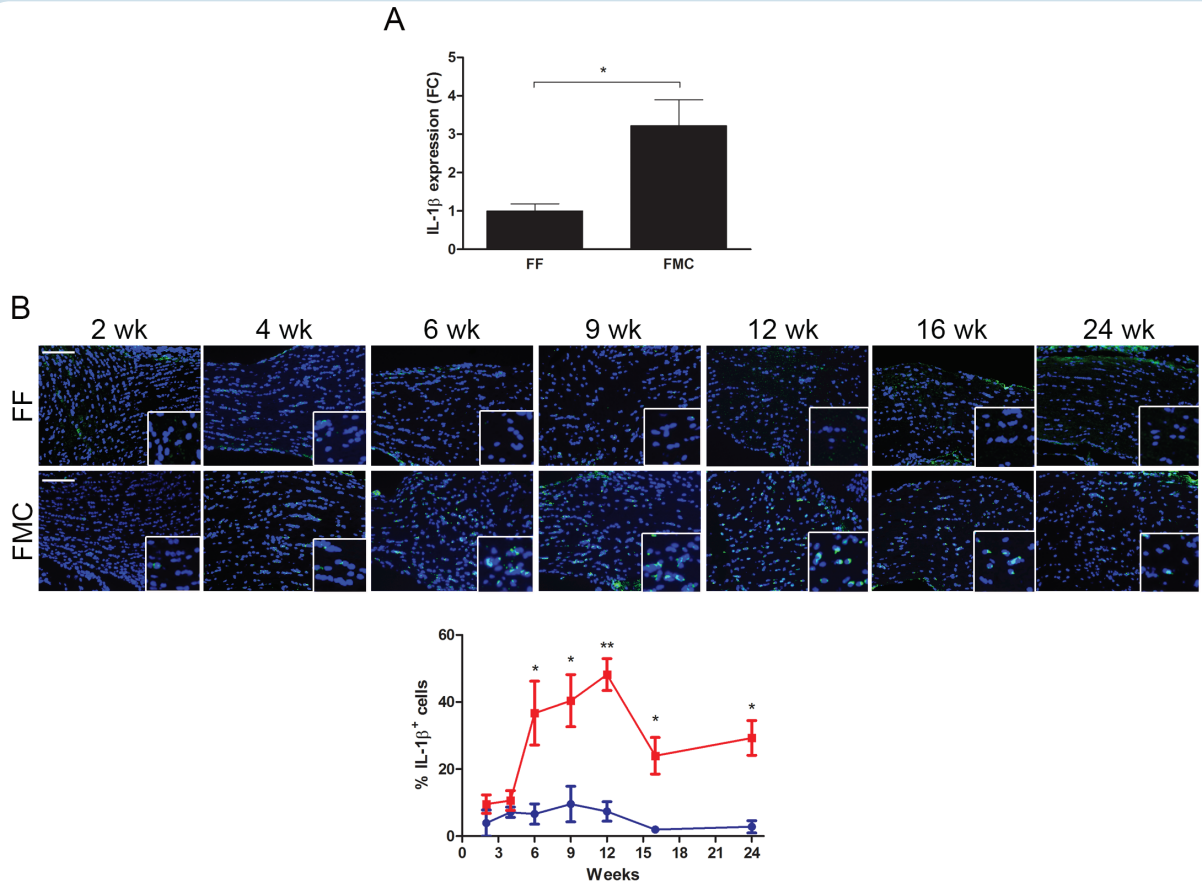

Fig. 5 *Nf1* optic glioma mice have more tumoral IL-1β expression. (A) The %IL-1β+ cells increased from 6 weeks to 12 weeks of age, but declined at 16 and 24 weeks of age. (B) Quantitative real-time PCR revealed 2.2-fold greater *Il1b* optic nerve RNA expression in 12-week-old FMC ($n = 5$) relative to FF ($n = 3$) mice. Data are represented as a fold change (FC) following normalization to *H3f3a* expression. *$P \leq .05$.

Brn3a+ cells (control, 60.1% ± 3.05; lovastatin, 87.13% ± 4.98; $P = .0009$) and RNFL thickness (control, 4.27 µm ± 0.72; lovastatin, 8.25 µm ± 0.39; $P = .0003$) 8 weeks following the cessation of treatment were similar to that observed in FMC mice maintained on lovastatin (Fig. 5C).

Discussion

In this study, we leveraged a well-studied GEM model of NF1 optic glioma to define the sequence of events that culminate in retinal dysfunction. Using this approach, we made several novel observations relevant to brain tumor pathogenesis and the evolution of visual impairment.

First, we show that the natural decline in optic nerve microglia content is blunted in the context of a developing optic glioma. The importance of microglia is underscored by the finding that 30%–50% of the cells in human NF1-associated or sporadic pilocytic astrocytomas are Iba1+ monocytes,[15] which in *Nf1* mouse optic gliomas are CD11b+;CD45^{low} microglia that express CX3CR1 important for optic gliomagenesis.[17] Moreover, microglia are critical for optic glioma maintenance, as genetic or pharmacological silencing of microglia function attenuates tumor growth.[15] This trophic effect is mediated by chemokines, notably Ccl5, such that Ccl5 neutralization reduces murine optic glioma proliferation in vivo.[29] It is therefore not surprising that elevated microglia numbers represent one of the earliest events in *Nf1* optic gliomagenesis, preceding the expansion of macroglial cells. Moreover, the normal loss of microglia in the optic nerve during development proceeds by apoptosis (Supplementary Fig. S3), a physiologic process that is attenuated in FMC mice.

Second, in addition to mediating gliomagenesis and continued tumor growth, microglia are important mediators of neuronal injury. In other nervous system disorders, microglia elaborate neurotoxic compounds that initiate axonal damage and neuronal loss.[30] One of these inflammatory agents, IL-1β, has been implicated in neuronal injury and death,[26] particularly in RGCs following neonatal hypoxia-ischemia.[31] We observed increasing IL-1β levels in the optic nerves of tumor-bearing relative

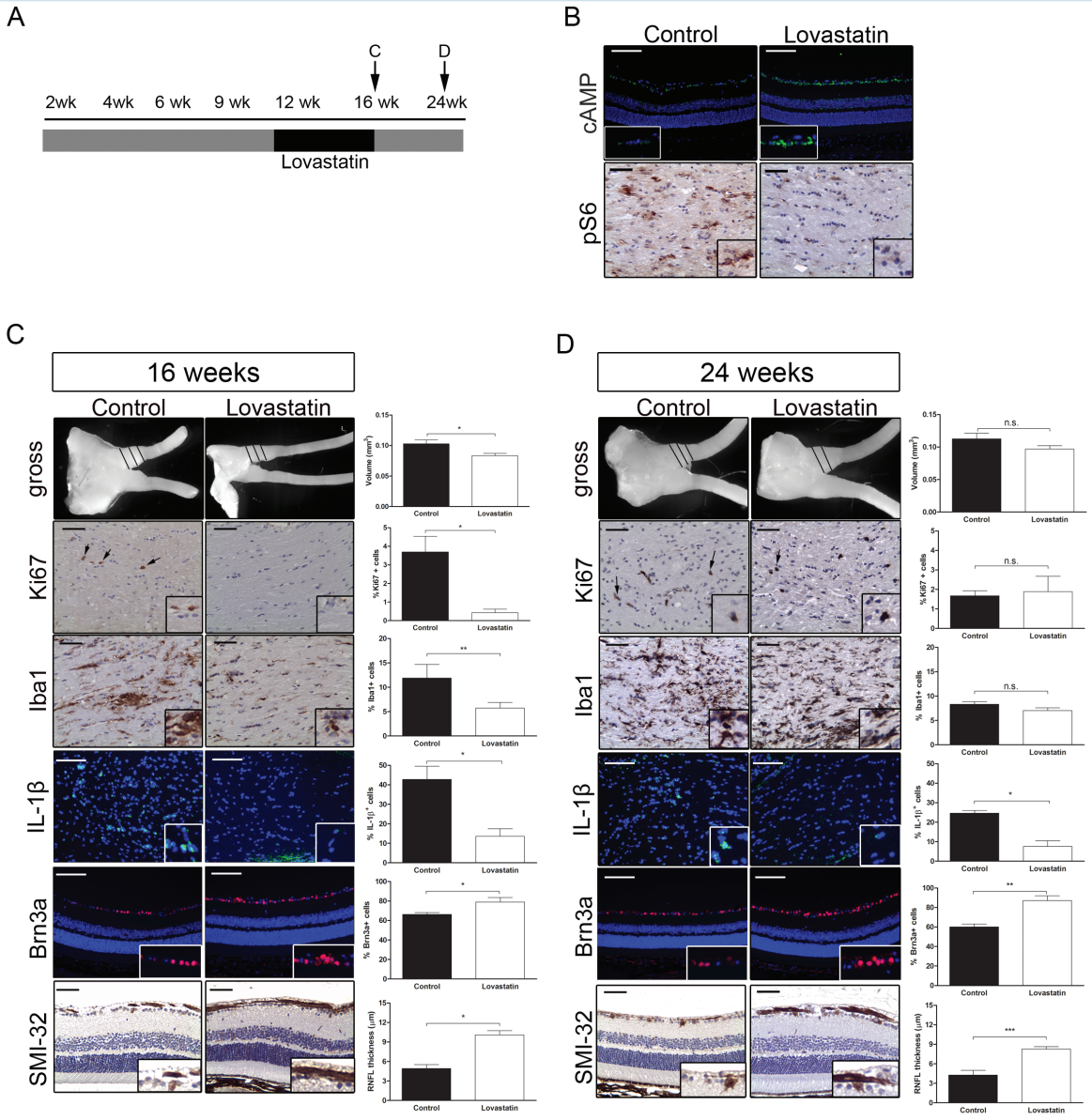

Fig. 6 Lovastatin attenuates retinal dysfunction. (A) Schematic of treatment schedule. (B) cAMP immunostaining in the RGC layer revealed increased cAMP levels (top) and decreased optic nerve $pS6_{Ser240/244}$ immunoreactivity (bottom) following lovastatin treatment compared with controls. (C) Lovastatin treatment decreased the volumes, %Ki67+ cells, %Iba1+ cells, and %IL-1β+ cells in FMC optic nerves compared with controls immediately following treatment cessation (16 wk of age). There was also an increase in the %Brn3a+ cells and RNFL thickness (SMI-32 immunohistochemistry). (D) Mice treated with lovastatin for 4 weeks and euthanized 8 weeks later showed no differences in optic nerve volumes, %Ki67+ cells, or %Iba1+ cells relative to controls; however, the %IL-1β+ cells was reduced, and the %Brn3a+ cells and RNFL thickness (SMI-32 immunohistochemistry) were increased. Black = vehicle, white = lovastatin, $*P \leq .05$,$**P \leq .01$, $P \leq .001$. Scale bars = 50 μm.

to control mice that coincided with the timing of microglia activation and RGC apoptosis, suggesting that this interleukin may partly drive the axonal damage program during tumor evolution. While formal proof for IL-1β as the essential mediator of optic glioma–mediated RGC damage is lacking, preliminary experiments have shown that minocycline inactivation of microglia results in reduced IL-1β expression (data not shown). Future experiments using IL-1β inhibitors will be required to demonstrate that this factor is the responsible neurotoxic agent in this setting. Nonetheless, the ability of microglia to both stimulate tumor expansion (Ccl5) and create neuronal injury (IL-1β) raises the intriguing possibility that future therapies targeting tumor-associated monocytes might attenuate optic glioma tumor growth and reduce retinal dysfunction.

Third, the correlation between OCT and RNFL thickness/RGC loss supports the use of this objective measure in

the assessment of retinal damage resulting from optic glioma. Previous studies have demonstrated that OCT is an accurate measure of RNFL thickness in rodent models, similar to our findings in *Nf1* optic glioma. Importantly, we report that RNFL thickness also strongly correlates with RGC loss, such that a RNFL thickness of <7.5 microns is predictive of >30% RGC loss, a threshold beyond which impairments in visual acuity are associated.[25] In this regard, reduced visual acuity is not observed in *Nf1* mutant mice until 6 months of age,[12] when RGC loss reaches 50%, providing a window for therapeutic intervention between the onset of RGC commitment to death and significant RGC dropout.

While there are notable differences in retina structure and composition between rodents and humans,[32] mice provide excellent experimental tools to identify the pathogenic mechanisms underlying human eye diseases.[33] Importantly, in the context of NF1-OPG, where surgical specimens of the optic nerve/retina are exceedingly rare, the use of validated preclinical models offers unique opportunities to carefully examine potential clinical biomarkers. As such, we detected RNFL thinning before the onset of vision loss, providing an objective measure of visual pathology critical for future preclinical (and later clinical) studies aimed at preventing further retinal pathology and vision loss.

Fourth, based on the concept that therapeutic intervention during a vulnerable window might attenuate further retinal pathology, we performed proof-of-concept experiments using lovastatin as a tool compound to target both RAS/mitogen–extracellular signal-regulated kinase (MEK)/Akt/mTOR-driven tumor growth and RAS/cAMP-mediated RGC survival. While treatments that inhibit phosphatidylinositol-3 kinase/Akt (MK2206[34]), MEK (PD0325901[34]), or mTOR (rapamycin[13]) signaling or therapies that suppress microglia function[16] each result in improvements in RGC survival and RNFL thickness, they do not directly target the signaling cascades controlled by the *NF1* protein (neurofibromin) important for RGC survival. RGC survival is mediated by cAMP[11] through RAS control of an atypical protein kinase C (PKCζ), such that lovastatin treatment of *Nf1* mutant neurons normalizes cAMP levels.[28] Consistent with neurofibromin/cAMP control of RGC survival in the setting of an optic glioma, treatment with rolipram to block phosphodiesterase-4–mediated cAMP degradation results in reduced RGC apoptosis in vivo.[11]

Using lovastatin, we observed a sustained preservation of RGC numbers and RNFL thickness 2 months following treatment cessation, at a time when tumor proliferation and volume had returned to pretreatment levels. The fact that we observed a durable effect suggests that short periods of treatment may be sufficient to attenuate the natural progression of events that drive vision loss. In this regard, raising cAMP levels and reducing IL-1β production when IL-1β expression and RGC apoptosis are maximal might blunt the effects of microglia-induced damage and neuronal death during this vulnerable interval, after which IL-1β levels and RGC apoptosis naturally decline. Further refinements using different treatment schedules and therapeutic agents will be required to optimize the interval during which maximal benefit to visual outcomes can be achieved.

Lastly, these results become increasingly more relevant in the context of emerging studies demonstrating that regeneration of RGC axons may be possible. While the mechanisms may be different, c-myc was identified as a key protein in RGC regeneration, such that overexpression of c-myc following optic nerve crush injury resulted in axon regeneration.[35] Other treatments that also ameliorate RGC death and promote axonal regeneration include insulin-like growth factor 1/ciliary neurotrophic factor administration[36] and enhanced conduction through the optic nerve.[37] Taken together, the discovery of a therapeutic window to attenuate further RGC loss establishes the foundations for future investigations in mice ultimately aimed at ameliorating visual decline in children with NF1-OPG.

Supplementary Material

Supplementary material is available at *Neuro-Oncology* online.

Funding

This work was supported by the Alex's Lemonade Stand Foundation and the National Cancer Institute (CA214146-01) to D.H.G. J.A.T. was supported by the Neurosciences T32 Training Grant (NS007205).

Conflict of interest statement. The authors have no conflicts to disclose.

References

1. Listernick R, Charrow J, Greenwald M, et al. Natural history of optic pathway tumors in children with neurofibromatosis type 1: a longitudinal study. *J Pediatr*. 1994;125(1):63–66.
2. Listernick R, Ferner RE, Liu GT, et al. Optic pathway gliomas in neurofibromatosis-1: controversies and recommendations. *Ann Neurol*. 2007;61(3):189–198.
3. Hyman SL, Shores A, North KN. The nature and frequency of cognitive deficits in children with neurofibromatosis type 1. *Neurology*. 2005;65(7):1037–1044.
4. Isenberg JC, Templer A, Gao F, et al. Attention skills in children with neurofibromatosis type 1. *J Child Neurol*. 2013;28(1):45–49.
5. Fisher MJ, Avery RA, Allen JC, et al.; REiNS International Collaboration. Functional outcome measures for NF1-associated optic pathway glioma clinical trials. *Neurology*. 2013;81(21 Suppl 1):S15–S24.
6. Zhu Y, Harada T, Liu L, et al. Inactivation of NF1 in CNS causes increased glial progenitor proliferation and optic glioma formation. *Development*. 2005;132(24):5577–5588.
7. Bajenaru ML, Hernandez MR, Perry A, et al. Optic nerve glioma in mice requires astrocyte Nf1 gene inactivation and Nf1 brain heterozygosity. *Cancer Res*. 2003;63(24):8573–8577.
8. Kim KY, Ju WK, Hegedus B, et al. Ultrastructural characterization of the optic pathway in a mouse model of neurofibromatosis-1 optic glioma. *Neuroscience*. 2010;170(1):178–188.

9. Banerjee D, Hegedus B, Gutmann DH, et al. Detection and measurement of neurofibromatosis-1 mouse optic glioma in vivo. *Neuroimage*. 2007;35(4):1434–1437.
10. Hegedus B, Hughes FW, Garbow JR, et al. Optic nerve dysfunction in a mouse model of neurofibromatosis-1 optic glioma. *J Neuropathol Exp Neurol*. 2009;68(5):542–551.
11. Brown JA, Gianino SM, Gutmann DH. Defective cAMP generation underlies the sensitivity of CNS neurons to neurofibromatosis-1 heterozygosity. *J Neurosci*. 2010;30(16):5579–5589.
12. Diggs-Andrews KA, Brown JA, Gianino SM, et al. Sex is a major determinant of neuronal dysfunction in neurofibromatosis type 1. *Ann Neurol*. 2014;75(2):309–316.
13. Hegedus B, Banerjee D, Yeh TH, et al. Preclinical cancer therapy in a mouse model of neurofibromatosis-1 optic glioma. *Cancer Res*. 2008;68(5):1520–1528.
14. Bajenaru ML, Garbow JR, Perry A, et al. Natural history of neurofibromatosis 1-associated optic nerve glioma in mice. *Ann Neurol*. 2005;57(1):119–127.
15. Simmons GW, Pong WW, Emnett RJ, et al. Neurofibromatosis-1 heterozygosity increases microglia in a spatially and temporally restricted pattern relevant to mouse optic glioma formation and growth. *J Neuropathol Exp Neurol*. 2011;70(1):51–62.
16. Daginakatte GC, Gutmann DH. Neurofibromatosis-1 (Nf1) heterozygous brain microglia elaborate paracrine factors that promote Nf1-deficient astrocyte and glioma growth. *Hum Mol Genet*. 2007;16(9):1098–1112.
17. Pong WW, Higer SB, Gianino SM, et al. Reduced microglial CX3CR1 expression delays neurofibromatosis-1 glioma formation. *Ann Neurol*. 2013;73(2):303–308.
18. Rosenfeld J, Dorman ME, Griffin JW, et al. Distribution of neurofilament antigens after axonal injury. *J Neuropathol Exp Neurol*. 1987;46(3):269–282.
19. Toonen JA, Anastasaki C, Smithson LJ, et al. NF1 germline mutation differentially dictates optic glioma formation and growth in neurofibromatosis-1. *Hum Mol Genet*. 2016;25(9):1703–1713.
20. Nadal-Nicolás FM, Jiménez-López M, Sobrado-Calvo P, et al. Brn3a as a marker of retinal ganglion cells: qualitative and quantitative time course studies in naive and optic nerve-injured retinas. *Invest Ophthalmol Vis Sci*. 2009;50(8):3860–3868.
21. Boylan KB, Glass JD, Crook JE, et al. Phosphorylated neurofilament heavy subunit (pNF-H) in peripheral blood and CSF as a potential prognostic biomarker in amyotrophic lateral sclerosis. *J Neurol Neurosurg Psychiatry*. 2013;84(4):467–472.
22. Natori A, Ogata T, Sumitani M, et al. Potential role of pNF-H, a biomarker of axonal damage in the central nervous system, as a predictive marker of chemotherapy-induced cognitive impairment. *Clin Cancer Res*. 2015;21(6):1348–1352.
23. Avery RA, Cnaan A, Schuman JS, et al. Longitudinal change of circumpapillary retinal nerve fiber layer thickness in children with optic pathway gliomas. *Am J Ophthalmol*. 2015;160(5):944–952 e941.
24. Dysli C, Enzmann V, Sznitman R, et al. Quantitative analysis of mouse retinal layers using automated segmentation of spectral domain optical coherence tomography images. *Transl Vis Sci Technol*. 2015;4(4):9.
25. Kerrigan-Baumrind LA, Quigley HA, Pease ME, et al. Number of ganglion cells in glaucoma eyes compared with threshold visual field tests in the same persons. *Invest Ophthalmol Vis Sci*. 2000;41(3):741–748.
26. Kaur C, Sivakumar V, Zou Z, et al. Microglia-derived proinflammatory cytokines tumor necrosis factor-alpha and interleukin-1beta induce Purkinje neuronal apoptosis via their receptors in hypoxic neonatal rat brain. *Brain Struct Funct*. 2014;219(1):151–170.
27. Li W, Cui Y, Kushner SA, et al. The HMG-CoA reductase inhibitor lovastatin reverses the learning and attention deficits in a mouse model of neurofibromatosis type 1. *Curr Biol*. 2005;15(21):1961–1967.
28. Anastasaki C, Gutmann DH. Neuronal NF1/RAS regulation of cyclic AMP requires atypical PKC activation. *Hum Mol Genet*. 2014;23(25):6712–6721.
29. Solga AC, Pong WW, Kim KY, et al. RNA sequencing of tumor-associated microglia reveals Ccl5 as a stromal chemokine critical for neurofibromatosis-1 glioma growth. *Neoplasia*. 2015;17(10):776–788.
30. Hambardzumyan D, Gutmann DH, Kettenmann H. The role of microglia and macrophages in glioma maintenance and progression. *Nat Neurosci*. 2016;19(1):20–27.
31. Sivakumar V, Foulds WS, Luu CD, et al. Retinal ganglion cell death is induced by microglia derived pro-inflammatory cytokines in the hypoxic neonatal retina. *J Pathol*. 2011;224(2):245–260.
32. Chang B. Mouse models for studies of retinal degeneration and diseases. *Methods Mol Biol*. 2013;935:27–39.
33. McKinnon SJ, Schlamp CL, Nickells RW. Mouse models of retinal ganglion cell death and glaucoma. *Exp Eye Res*. 2009;88(4):816–824.
34. Kaul A, Toonen JA, Cimino PJ, et al. Akt- or MEK-mediated mTOR inhibition suppresses Nf1 optic glioma growth. *Neuro Oncol*. 2015;17(6):843–853.
35. Belin S, Nawabi H, Wang C, et al. Injury-induced decline of intrinsic regenerative ability revealed by quantitative proteomics. *Neuron*. 2015;86(4):1000–1014.
36. Duan X, Qiao M, Bei F, et al. Subtype-specific regeneration of retinal ganglion cells following axotomy: effects of osteopontin and mTOR signaling. *Neuron*. 2015;85(6):1244–1256.
37. Bei F, Lee HH, Liu X, et al. Restoration of visual function by enhancing conduction in regenerated axons. *Cell*. 2016;164(1–2):219–232.